Wall Effects: A Case Study on Terminal Falling Velocity of Spherical Particles Moving in a Carreau Model Fluid

Ali Amiri

Mechanical Engineering Department, Heat and Fluid, Isfahan, Iran
Amiriali144@yahoo.com

Abstract: In this work we presented an experimental verification of a numerical simulation of wall effects on the terminal falling velocity of spherical particles moving along the axis of a cylindrical vessel filled with a Carreau model fluid. Using a finite element method, we obtained dependences of the wall correction factor FW on the sphere to tube ratio d/D and on the dimensionless Carreau model parameters m, Λ, and ηr and then we compared calculated data of the wall correction factor with the results of our falling sphere experiments. The experiments were carried out in six types of cylindrical Perspex columns (16 mm, 21 mm, 26 mm, 34 mm, 40 mm, and 90 mm in diameter) filled with aqueous solutions of polymers showing different degrees of shear thinning and elasticity. Seventeen types of spherical particles (1 to 8 mm in diameter) made of following materials: glass, ceramics, steel, lead, and tungsten carbide, were used for drop test. Measurements of the liquid flow curves, primary normal stress differences, oscillatory, creep and recovery, stress relaxation, and stress growth tests were carried out on the rheometer Haake MARS (Thermo Scientific). A good agreement between numerically and experimental FW data was observed.
[Ali Amiri. **Wall Effects: A Case Study on Terminal Falling Velocity of Spherical Particles Moving in a Carreau Model Fluid .** *Researcher* 2017;9(10):75-80]. ISSN 1553-9865 (print); ISSN 2163-8950 (online). http://www.sciencepub.net/researcher. 12. doi:10.7537/marsrsj091017.12.

Keywords: wall effect, sphere free fall, Carreau viscosity model, drag coefficient

1. Introduction

Knowing about the terminal falling velocity of a rigid particle is necessary for the solution of numerous theoretical and practical problems such as, design calculations of thickeners, fluidized bed equipment, pipeline transport systems, falling particle viscometry, and so on. Studying the influence of fluid non-Newtonian behavior of the fall of a particle (particularly a sphere) is one of the most important issues from the middle of the 20th century. Chhabra (2006), in his book, provided a comprehensive review of literature and an analysis of the present state of investigation of this problem along with a short review of the calculation of the drag coefficient of particles falling in Newtonian fluids. The majority of efforts have been paid to investigate creeping flow of purely viscous fluids around a sphere. In order to solve this flow, fluid viscosity models containing zero shear viscosity as a parameter are preferred. Such a widely used viscosity model is the four-parameter Carreau model with parameters η0 (zero-shear rate viscosity), η∞ (infinite shear rate viscosity), λ, and m:

$$\frac{\eta - \eta_\infty}{\eta_0 - \eta_\infty} = [1 + (\lambda\dot{\gamma})^2]^{\frac{m-1}{2}} \quad (1)$$

The benefit of above equation is the ability to describe the viscosity, η, in a wide range of shear rates with very good accuracy.

The problem of the evaluation of the drag coefficient of a sphere falling freely in an unbounded Carreau model fluid has been solved numerically by Chhabra and Uhlherr (1980), Bush and Phan-Thien (1984), and Doleček et al. (1990). Impact of the dimensionless viscosity parameter

$$= \frac{\eta - \eta_\infty}{\eta_0 - \eta_\infty} \quad (2)$$

On the drag of a sphere has been solved by Doleček et al. (2004). Calculating the sphere terminal falling velocity, based on relationships approximating the results determined by Doleček et al. (1990) for $\eta_r = 1$, was provided by Machač et al. (2000).

It is well known that, the confining walls will cause an extra retardation force on a particle falling in a viscous fluid because of the upward flux of the fluid displaced by the particle. The effect of container walls is usually expressed using the wall correction factor F_W which can be defined as:

$$F_W = \frac{U}{U_\infty} \quad (3)$$

Where, U/U_∞ is the ratio of the terminal falling velocity in a bounded fluid to that in an unbounded one.

For a spherical particle moving slowly and axially through an incompressible Newtonian fluid in a cylindrical container, the wall correction factor, F_W, is a function of the sphere to tube diameter ratio, $\beta = d/D$ and for non-Newtonian fluids, additional dimensional groups appear depending on the selected rheological model. The majority of information on the wall effects, particularly for non- Newtonian fluids, is based mainly on experiments.

Only limited theoretical and numerical investigations of the effects of containing walls on the

sphere motion in purely viscous fluids without a yield stress have been conducted (Chhabra, 2006). Missirlis et al. (2001) conducted a numerical study of the wall effects on the terminal velocity of a sphere falling freely via a power-law fluid at the axis of a cylindrical tube in the creeping flow system. This solution has been adjusted by Song et al. (2009) for sphere Reynolds numbers of 1–100. To test the possibility of using the COMSOL Multiphysics software for steady non-Newtonian flows to solve the flow of purely viscous fluids around a solid obstacle, the effect of containing walls on sphere motion in a power-law fluid was recalculated by this software package (Strnadel & Machač, 2008). Their results were in very good agreement with the data published by Missirlis et al. (2001). Moreover, while the theory predicts a strong impact of the power law index, n, on the wall factor, the existing experimental data do not confirm this fact. Given that, the power law viscosity model can be successfully used for the approximation of the fluid viscosity function only in a quite narrow region of the shear rate, the creeping flow over a solid sphere in a cylindrical tube was solved for a Carreau model fluid using the finite element method benefitting the above mentioned COMSOL Multiphysics software (Strnadel & Machač, 2009a; Machač et al., 2009). The suitability of the relationship approximating the results of these numerical calculations obtained for $\beta = 0$ was tested for fall of spherical particles within viscoelastic fluids by Strnadel & Machač (2009b). In the paper, the relationships valid for $0 \le \beta \le 0.5$ were suggested and their usability was tested by comparing the calculated wall factor data with the results of our new extensive set of falling sphere experiments in polymer solutions showing different degrees of shear thinning and elasticity.

2. Material and Methods

2.1. Principles

Numerical solution of the mathematical model provided in (Strnadel & Machač, 2009a; Machač et al, 2009) resulted in the velocity, pressure, and stress fields. The magnitude of the drag force, F_D, on the sphere and the resulting drag coefficient, C_D, were the main outputs for further investigation:

$$C_D = \frac{|F_D|}{\pi \frac{D^2}{4} \frac{1}{2} \rho U^2} \quad (4)$$

Where d is the sphere diameter, ρ is the density of the fluid, and U is the sphere terminal falling velocity.

The drag coefficient, C_D, for the creeping flow of a Carreau model fluid around a sphere is expressed as:

$$C_D = \frac{24}{Re_0} X(\eta_r, \Lambda, m, \beta) \quad (5)$$

Where,

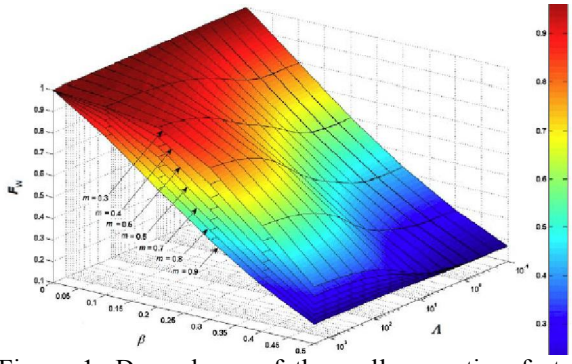

Figure 1: Dependence of the wall correction factor FW on β, m, and Λ for $\eta_r = 1$

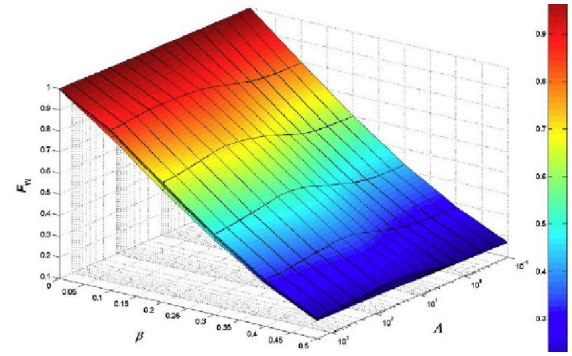

Figure 2: Dependence of the wall correction factor F_W on β, m, and Λ for $\eta_r = 0.75$

$$Re_0 = \frac{Ud\rho}{\eta_0} \quad (6)$$

is the Reynolds number based on the zero-shear rate viscosity and X is the corrective factor of drag coefficient depending on the Carreau model parameter, m, the dimensionless time parameter Λ, and the ratios η_r and β. By comparing Eq. (4) with Eq. (5) we have

$$X(\eta_r, \Lambda, m, \beta) = \frac{|F_D|}{6\pi\eta_0 RU} \quad (7)$$

Then the wall correction factor, F_W, (Eq. 3) is:

$$F_W(\eta_r, \Lambda, m, \beta) = \frac{X_\infty}{X} \quad (8)$$

To calculate factor X, an iterative solution was used for such velocity, $U < U\infty$, where the drag force is $FD = FD\infty$ (Strnadel & Machač, 2009a).

Dependences of FW = f (β, m, Λ) calculated for $\eta_r = 1$ and 0.75 are exhibited in Figures 1 and 2.

The wall correction factor, F_W, is fully dependent on ratio β. The dependence of F_W on m and Λ varies based on the value of the viscosity parameter η_r. For $\eta_r \rightarrow 1$, the theoretical estimates of FW are largely depended on m and Λ. At the same time, the wall effect becomes less significant with the decreasing values of m and increasing values of Λ. By the decrease of the values for η_r, the dependence of FW

on m and Λ decreases and the dependence of FW on Λ show a local maximum.

Table 1: Composition of the model liquids

Liquid symbol	Polymer	Composition/mass %
L1	Carboxymethylcellulose (CMC)	1.2
L2	Hydroxyethylcellulose (Natrosol 250 HHX)	1.0
L3	Methylcellulose (Tylose)	3.0
L4	Polyacryl amide (Separan 45)	1.2
L5	Polyacryl amide (Hercofloc 818)	0.8
L6	Polyacryl amide (Kerafloc KX4026)	0.75
L7	Polyacryl amide (Praestol 2540)	0.4
L8	Polyethelene oxide (Polyox WSR 303)	1.2
L9	Polyalkylene glycol (Emkarox HV45)/CMC	35/0.02
L10	Polyalkylene glycol (Emkarox HV45)/CMC	35/0.04
L11	Polyalkylene glycol (Emkarox HV45)/CMC	35/0.08
L12	Polyalkylene glycol (Emkarox HV45)/CMC	35/0.16

When dimensionless time $\Lambda \rightarrow 0$ or m = 1, then the calculated value for FW will be reduced to the Newtonian correlation, which is in accordance with the viscosity function since the Carreau model (Eq. (1)) predicts constant viscosity i.e. $\eta = \eta_0$. The identical situation arises for high values of the product $\lambda\dot{\gamma}$, when behavior of the Carreau liquid rheological approaches that of a Newtonian liquid with viscosity equal to η_∞. Given this fact, the existence of the aforementioned maximum can be described as the wall factor values are lower for Newtonian fluids than for shear thinning liquids.

For simplification of the computations to determine the wall factor, F_w, a relationship approximating the numerically calculated data X (η_r, m, Λ, β) was used. By optimizing the resulted numerical data, it was found that, the following relationship can be used to predict factor X in the intervals: $0.3 \leq \eta_r \leq 1$, $0.3 \leq m \leq 1$, $0.1 \leq \Lambda \leq 2000$, and $0 \leq \beta \leq 0.5$.

$$\frac{X - X_\Lambda^\infty}{X_\Lambda^0 - X_\Lambda^\infty} = \left[1 + (K_1\Lambda)^{k_2}\right]^{\frac{k_3-1}{k_2}} \quad (9)$$

The limiting values of X for $\Lambda = 0$ and $\Lambda \rightarrow \infty$ are as the following.

$$X_\Lambda^0 = \frac{1}{1 - (1 + 1.0526)\beta + (1 + 0.5876)\beta^2} \quad (10a)$$

$$X_\Lambda^\infty = \frac{1 - \eta_r}{1 - (1 + 1.0526)\beta + (1 + 0.5876)\beta^2} \quad (10b)$$

Moreover, the parameters k1–k4 (Eq. (9) are as the following.

$$k_1 = -0.1272(\beta + 1)(\eta_r + 1)m + 0.9348\beta(1 - \beta) + 0.4127 \quad (10c)$$

$$k_2 = [0.9348(\beta - 1) - 0.3624](1 - \eta_r)m + 1.4101(\beta + 1) \quad (10d)$$

$$k_3 = [0.9348(\beta - 1)(1 - \eta_r) + 0.3624\eta_r](1 - m) + 0.4127m + 0.5876 \quad (10e)$$

$$k_4 = [0.9348(\beta - 1) + 0.5876](\eta_r - 1)m - \eta_r(1 + \beta) + 1.0727 \quad (10f)$$

The mean relative deviation between the data determined based on the Eq. (9) and Eq. (10) and those calculated numerically are only 0.8 %. The observed maximum deviations (6–9.3 %) were for $\eta_r = 1$, m = 0.3, and β > 0.3.

2.2. Experimental setup

Falling sphere experiments were performed in six cylindrical Perspex columns filled with aqueous solutions of different polymers. The columns were placed

in thermostatic water bath and tempered at 23.0◦C. Diameters of the columns were 16 mm, 21 mm, 26 mm, 34 mm, 40 mm, and 90 mm, which lead to ratio $\beta \in \beta \in \langle 0.011;\ 0.499 \rangle$. Polymer solutions L1–L8 were prepared by dissolution of powdered polymers in demineralized water; solutions L9–L12 by dissolution of the appropriate amount of powdered carboxy methyl cellulose (CMC) in aqueous solutions of poly alkylene glycol Emkarox HV45. Table 1 shows the composition of the test liquids and their densities, and table 2 shows Carreau model parameters. Seventeen types of spherical particles of glass, ceramics, steel, lead, and tungsten carbide were used for the drop tests. Table 3 shows the characteristics of the test particles.

The range of terminal falling velocities, U_{exp}, in these experiments was from 0.063 mm s^{-1} to 202 mm s^{-1}, which is in agreement with the Reynolds number interval from 2.52×10^{-6} to 2.64 and to the dimensionless time parameter interval from 0.129 to 1423. Time interval between individual drop tests was set at least five minutes to avoid the occurrence of a "depleted region" in the liquid.

Table 2: Characteristics of the model liquids

Liquid symbol	Density	Carreau model (Eq. (1)) parameters (23 °C)				
	ρ/(kg m^{-3})	H_0/(Pa s)	η_∞/(Pa s)	λ/s	m	η_r
L1	1002	6.103	0.001	2.16	0.509	1.000
L2	1000	4.301	0.001	0.999	0.470	1.000
L3	1006	6.965	0.001	0.290	0.610	1.000
L4	1002	17.92	0.001	12.7	0.424	1.000
L5	1000	63.50	0.001	34.5	0.310	1.000
L6	1002	23.71	0.001	22.0	0.317	1.000
L7	999.3	18.71	0.001	11.0	0.278	1.000
L8	1000	3.864	0.001	4.08	0.512	1.000
L9	1055	0.644	0.326	3.24	0.787	0.508
L10	1055	0.876	0.284	2.04	0.752	0.676
L11	1055	1.418	0.261	1.79	0.729	0.816
L12	1047	1.675	0.116	1.57	0.691	0.931

Table 3: Characteristics of the test spherical particles

Symbol	Diameter D/mm	Density P_s/(kg m^{-3})	Symbol	Diameter D/mm	Density P_s/(kg m^{-3})
S1	1.93	2525	S10	7.99	3908
S2	3.13	2486	S11	0.99	15119
S3	4.12	2597	S12	1.49	15119
S4	4.93	2508	S13	1.99	15119
S5	6.12	2495	S14	2.99	15119
S6	1.99	3908	S15	0.99	7526
S7	2.99	3908	S16	3.17	7789
S8	3.99	3908	S17	2.00	11118
S9	5.99	3908			

Assessment of liquid flow curves, primary normal stress differences, oscillatory, creep and recovery, stress relaxation, and stress growth tests were performed at 23.0◦C on a rheometer Haake MARS (Thermo Scientific, Germany).

3. Results

3.1. Rheological measurements

Liquid viscosity functions calculated from experimentally obtained flow curves were estimated by the four-parameter Carreau model with a very good accuracy. Figure 3 shows an example of the viscosity function course of some model fluids.

As it appear from the creep and recovery tests (Fig. 4), polymer solutions L1–L3 and L9–L12 show only slight linear elasticity. On the opposite side, fluids L4–L7 (poly acryl amide solutions) exhibited strong linear elasticity. Somewhat weaker elasticity was observed in fluid L8 (solution of polyethylene oxide). Similar results were obtained from the oscillatory and stress relaxation measurements. It is worth mentioning that, the degree of linear elasticity of the test fluids corresponds with the values of parameter λ of the Carreau viscosity model (Table 2). Measurements of the primary normal stress difference, N_1, showed that, the rate of non-linear elasticity of the test fluids L1, L2, L4–L7, and L9–L12 are in agreement with the above-mentioned fluid linear elasticity.

3.2. Wall factor

Values of $U_{\infty,exp}$ of the terminal falling velocities in unbounded fluid were obtained by linear extrapolation of the experimental dependences U_{exp} vs. β to the value of $\beta \rightarrow 0$. For extrapolation, interval $\beta \in (0; 0.2)$ where the dependences of U_{exp}= f (β) were nearly linear, was selected. Using terminal falling velocities, $U_{\infty,exp}$, experimental values, $F_{W,exp}$, of the wall correction factor were calculated from Eq. (3) and then compared with the corresponding values, $F_{W,cal}$, obtained according to Equations (8)–(10).

Figure 3: Dependence of the wall factor F_W on the ratio β for model liquid L10, η_r=0.676, m = 0.512, $\Lambda \in (4.33; 271.2)$, n = 0.873; (○ – calculated values), (●– experimental values), (—- Haberman and Sayre (1958)), (—- power law model).

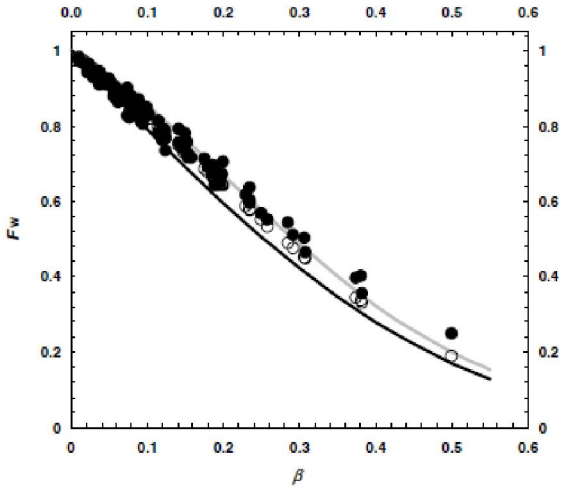

Results of the comparison for liquids L1, L5, and L10 are exhibited in Figures 3. These figures show that, experimental values of the wall factor were in a good agreement with the calculated results. Diagrams for the other test fluids were identical. The mean relative deviation between $F_{W,exp}$ and $F_{W,cal}$ data determined for the whole set of experiments was 3.9 %. Higher amounts of deviations (6–23 %) were observed for the ratio of $\beta > 0.37$. They can be partly as the results of experimental errors in the terminal falling velocity measurements in narrow columns when the strictly axial position of falling spheres is not easily obtainable and partly by the previously mentioned lower accuracy of the approximation formula (Eq. (10)) for $\beta > 0.3$. It is also worth mentioning that, the elasticity of test liquids L4–L8 did not largely affect the wall effects.

For comparison, dependences F_W = f (β) obtained from the relationship of Haberman and Sayre (1958):

$$F_W = \frac{1 - 2.105\beta - 1.706\beta^3 + 0.72603\beta^6}{1 - 0.75857\beta^5} \quad (11)$$

This relation is valid for Newtonian fluids. The following relationship

$$F_W = \frac{1}{1 + a_1\beta^2 + a_2\beta^2 + a_3\beta^3 + a_4\beta^4} \quad (12)$$

estimates the dependence F_W = f (β) calculated numerically for power law fluids by Missirlis et al. (2001) and Strnadel and Machač (2008) that displayed in Figures 6–8. Parameters a_1 to a_4 are given by the following polynomial functions (Strnadel & Machač, 2008).

$$a_1 = 4.317n^2 - 2.963n \quad (13a)$$
$$a_2 = 4.317n^2 + 4.827n + 4.827 \quad (13b)$$
$$a_3 = -66.09n^2 + 660.9n - 38.80 \quad (13c)$$
$$a_4 = 84.44n^2 - 66.09n + 66.09 \quad (13d)$$

It is obvious that, container walls have smaller effect on the particle movement in shear thinning fluids than in Newtonian fluid. However, Eq. (12), based on the power law model, predicts for liquids characterized by flow index n < 0.8 higher values of F_W compared to the experimental results.

4. Discussions

The results of our numerical simulation of the wall effects on the terminal falling velocity of spherical particles moving slowly (creeping flow system) in a cylindrical vessel filled with Carreau model fluid are presented. Via optimizing the obtained numerical data, the relationships (Eq. (9) and Eq. (10)) approximating the results of numerical solution of the drag coefficient corrective factor X were obtained. Validity of Eq. (9) and Eq. (10) was evaluated by comparing the wall factor data predicted using these equations with the results of our falling sphere experiments. The experiments were performed in six types of cylindrical Perspex columns filled with aqueous solutions of polymers showing different degrees of shear thinning and elasticity. Seventeen types of spherical particles of glass, ceramics, steel, lead, and tungsten carbide were used for the drop tests. A good agreement between the calculated and experimentally obtained F_W data was observed, which confirms the applicability of the proposed relationship for the wall effects calculation. The mean relative deviation between these data was only 3.9 %. It was also shown that, the container walls have smaller effect on the particle movement in shear thinning fluids than in Newtonian fluids. similarily, it was seen that, elasticity of the viscoelastic test liquids does not largely affect the wall effects.

Symbols

- a1–a4 parameters, Eqs. (12) and (13)
- C_D sphere drag coefficient
- d sphere diameter (m)
- D test column diameter (m)
- F_D drag force (N)
- $F_{D,\infty}$ drag force in an unbounded fluid (N)
- F_W wall correction factor
- $F_{W,cal}$ calculated experimental wall correction factor
- $F_{W,exp}$ experimental wall correction factor
- J creep compliancy (Pa^{-1})
- k1–k4 parameters, Eqs. (9) and (10)
- m dimensionless parameter of the Carreau model
- N1 first normal stress difference (Pa)
- R_{e0} Reynolds number, Eq. (6)
- t time (s)
- U terminal falling velocity in a test column ($m\ s^{-1}$)
- U_∞ terminal falling velocity in an unbounded fluid ($m\ s^{-1}$)
- U_{exp} experimental terminal falling velocity in a test column ($m\ s^{-1}$)
- $U_{\infty,exp}$ experimental terminal falling velocity in an unbounded fluid ($m\ s^{-1}$)
- X drag coefficient corrective factor, Eqs. (5), (7), and (8)
- X_∞ drag coefficient corrective factor for the fall in an unbounded fluid, Eq. (8)
- X_Λ^0 factor X for $\Lambda = 0$
- X_Λ^∞ factor X for $\Lambda \rightarrow \infty$
- β sphere to tube diameter ratio (= d/D)
- $\dot{\gamma}$ shear rate (s^{-1})
- η shear viscosity (Pa s)
- η_0 Carreau model parameter (zero-shear rate viscosity) Pa s
- η_r dimensionless relative viscosity (= $1 - \eta\infty/\eta 0$)
- η_∞ Carreau model parameter (infinite shear rate viscosity) (Pa s)
- Λ dimensionless time parameter (= $2\lambda U\infty/d$)
- λ Carreau model time parameter s
- ρ liquid density kg m−3
- ρ_s sphere density kg m−3

Corresponding Author:
Ali Amiri
E-mail: Amiriali144@yahoo.com

References

1. Bush, M. B., & Phan-Thien, N. (1984). Drag force on a spere in creeping motion through a Carreau model fluid. Journal of Non-Newtonian Fluid Mechanics, 16, 303–313. DOI: 10.1016/0377-0257(84)85016-8.
2. Chhabra, R. P. (2006). Bubbles, drops, and particles in non- Newtonian fluids (2nd ed., pp. 49–201 and 521–554). Boca Raton, FL, USA: CRC Press.
3. Chhabra, R. P., & Uhlherr, P. H. T. (1980). Creeping motion of spheres through shear-thinning elastic fluids described by the Carreau viscosity equation. Rheologica Acta, 19, 187–195. DOI: 10.1007/BF01521930.
4. Doleček, P., Bendová, H., Šiška, B., & Machač, I. (2004). Fall of spherical particles through a Carreau fluid. Chemical Papers, 58, 397–403.
5. Haberman, W. L., & Sayre, R. M. (1958). David Taylor Model Basin. Washington, DC, USA: U.S. Navy Department. (Report No. 1143).
6. Machač, I., Šiška, B., & Machačová, L. (2000). Terminal falling velocity of spherical particles moving through a Carreau model fluid. Chemical

Engineering and Processing, 39, 365– 369. DOI: 10.1016/S0255-2701(99)00101-4.
7. Machač, I., Strnadel, J., & Surý, A. (2009). Wall effects on a single spherical particle moving through a Carreau model fluid. In Novel Trends in Rheology III: Proceedings of the International Conference, 24 July 2009 (AIP Conference Proceedings, Vol. 1152, pp. 110–119). Zlín, Czech Republic. DOI: 10.1063/1.3203259.
8. Missirlis, K. A., Assimacopoulos, D., Mitsoulis, E., & Chhabra, R. P. (2001). Wall effects for motion of spheres in powerlaw fluids. Journal of Non-Newtonian Fluid Mechanics, 96, 459–471. DOI: 10.1016/S0377-0257(00)00189-0.
9. Song, D., Gupta, R. K., & Chhabra, R. P. (2009). Wall effects on a sphere falling in quiescent power law fluids in cylindrical tubes. Industrial & Engineering Chemistry Research, 48, 5845–5856. DOI: 10.1021/ie900176y.
10. Strnadel, J., & Machač, I. (2008). Wall effects on a single spherical particle moving through a power-law fluid. Scientific Papers of the University of Pardubice. Series A, 14, 107–120.
11. Strnadel, J., & Machač, I. (2009b). Fall of spherical particles in viscoelastic fluids. In Novel Trends in Rheology III: Proceedings of the International Conference, 24 July 2009 (AIP Conference Proceedings, Vol. 1152, pp. 110–119). Zlín, Czech Republic. DOI: 10.1063/1.3203286.
12. Strnadel, J., & Machač, I. (2009a). Wall effects on a single spherical particle moving through a Carreau model fluid. Scientific Papers of the University of Pardubice. Series A, 15, 175–185.

10/18/2017